



## ISTITUTO NAZIONALE DI RICERCA METROLOGICA Repository Istituzionale

Flow leaks normalization

*Original*

Flow leaks normalization / Spazzini, Pier Giorgio; La Piana, Gaetano; Piccato, Aline; Delnegro, Vittorio; Viola, Massimo. - In: MEASUREMENT. - ISSN 0263-2241. - 221:(2023).  
[10.1016/j.measurement.2023.113429]

*Availability:*

This version is available at: 11696/78979 since: 2024-02-21T11:46:35Z

*Publisher:*

ELSEVIER SCI LTD

*Published*

DOI:10.1016/j.measurement.2023.113429

*Terms of use:*

This article is made available under terms and conditions as specified in the corresponding bibliographic description in the repository

*Publisher copyright*

(Article begins on next page)



## Flow leaks normalization

Pier Giorgio Spazzini<sup>\*</sup>, Gaetano La Piana, Aline Piccato, Vittorio Delnegro, Massimo Viola

INRIM, Strada delle Cacce 91, I-10137 Torino, Italy

### A B S T R A C T

Flow leaks are small devices generating a well-determined flow when subject to a pressure differential (feed pressure).

Though, they need to be calibrated against a reference flow based on the feed pressure and fluid density through a complex relation derived from the modified Darcy law, therefore results of a calibration performed in a given condition are not necessarily valid when the leak is used in different conditions.

In this paper we will describe a correct renormalization of the calibration results allowing to compute precisely the actual flow rate generated by the leak.

A mathematical description of the renormalization will be presented and a method for the experimental determination of the permeability will be discussed.

It will be shown that the calibration uncertainty can be reduced by applying the correct normalization, and that the in-use uncertainty can be brought to be of the same order of magnitude as the calibration uncertainty.

### 1. Introduction

Flow leaks are small devices aimed at regulating the quantity of gas that flows through them (flow rate) by changing the pressure difference to which they are subject; since they allow to easily generate a well-defined flow and they are very stable, they are widely employed in several industrial fields, ranging from checks of leaks in flow rate devices to chemical applications, to food processing, textile permeability checks and so on.

The flow range of these devices is extremely large, ranging from fractions of an SCCM (Standard Cubic Centimetre per Minute) to hundreds of SLM (Standard Litres per Minute), depending on the size and fabrication process of the leak.

Two main technologies are applied for the manufacturing of the leaks active element: for small flow rates, the permeable element is produced by high-pressure sintering of ceramic or metallic materials, while for larger flow rates calibrated holes are drilled through very hard materials (synthetic rubies or similar); the active element is then inserted into a holder provided with standard gas connections which allows to insert the leak into the flow circuit.

Of course, the nominal flow rate through the leak is determined by design, but due to the uncertainties in the production process the actual value of the flow at a given pressure difference may vary for different leaks of the same model; for high-accuracy applications it is therefore necessary to calibrate the individual leak against a reference flow; also, such devices are often included within a Quality Management System (QMS), which again requires periodical calibration of the instruments.

In the present paper we will focus on the calibration of sintered leaks; an accurate analysis of the response of these devices shows that the flow rate depends not only on the pressure difference, but also on the feed pressure and on the fluid density, therefore a correct calibration, and a correct employment of its results, requires to take into account such influences.

To do this, we will describe the theoretical analysis of the renormalization of the calibration results, which when applied will allow to precisely compute the actual flow rate through leaks both in calibration and in use.

The analysis, fully described in Par. 2, is based on different forms of the Darcy law; such equation includes several parameters which are difficult, if not impossible, to know a priori, therefore an experimental determination of the coefficients is necessary. We will describe the experiments that we performed to this aim in par. 3, while in Par. 4 we will present the data analysis alongside to a few application examples.

### 2. Mathematical formulation

#### 2.1. Background and notation

The sintered block that constitutes the active element of the leak can be considered as a microporous element, i.e. a conglomeration of very small channels through which the gas flows. Due to the fluid dynamical drag generated within the channels, the gas undergoes a pressure drop (i.e., the pressure difference across the leak) which of course, at steady state, must be in equilibrium with the flow, hence the working principle

<sup>\*</sup> Corresponding author at: C/o INRIM – Strada delle Cacce, 91 – 10137 Torino, Italy.

E-mail address: [p.spazzini@inrim.it](mailto:p.spazzini@inrim.it) (P.G. Spazzini).

of the device.

The analysis presented here is based on the one performed in the paper by Carrigy et al. [1], slightly modified to adapt it to our needs; we will use the following symbols to describe the various quantities:

$A_{ex}$	is the exit section of the leak;
$B_v$	is the viscous permeability;
$c_1^k, c_2^k$	are constants that depend on the gas and on the channel;
$D^k$	is the Knudsen diffusivity;
$d_p^{eff}$	is the effective pore diameter;
$\eta$	is the gas dynamic viscosity;
$Kn$	is the Knudsen number;
$L$	is the length of the porous medium (active length of the leak in our case);
$M$	is the molar mass of the gas;
$N$	is the molar flux;
$Q_V$	is the volumetric gas flow;
$Q_{SCCM}$	is the gas flow in SCCM;
$\rho$	is the gas density;
$R$	is the radius of a capillary;
$R^*$	is the universal gas constant;
$T$	is the temperature;
$p$	is the pressure;
$v$	is the average velocity downstream of the leak;
$x$	is the spatial coordinate taken as positive;

the subscripts 1 and 2 refer to the conditions upstream and downstream of the leak, respectively, while the subscript  $ref$  refers to the reference conditions of interest.

## 2.2. Continuum vs molecular flow regimes

In order to better understand what follows, we recall here the basic concepts of flow regimes. A complete treatment of the topic is beyond the scopes of the present paper, but the interested reader can refer to [5] to go into more detail.

It is well known that fluids are composed of molecules, whose movements and interactions account for all the flow properties and phenomena. The immensely large number of molecules make it impossible to analyse such movements directly, but statistical analysis shows that, on a macroscopic level, the flow can be analysed through a set of partial differential equations (Navier-Stokes equations), provided that there is a sufficient number of molecules within the smallest significant volume of a flow. The significance of the volume is quantified using the Knudsen number ( $Kn$ ), defined as the ratio between the molecular mean free path and a relevant dimension of the problem at hand. This parameter clearly describes the significance of the flow volume with respect to the molecules; indeed, when the mean free path is of the same order as the dimension of the problem, there is a finite probability that a molecule does not interact with other molecules in between two interactions with the limiting walls; on the other hand, when  $Kn$  is extremely small, a molecule will encounter a large number of molecular collisions before an interaction with the wall, therefore averaging out all effects and rendering the medium effectively continuous.

It is generally assumed (see e.g. [1]) that when  $Kn < 0.001$  the flow can be considered as a continuum and that the so-called “no-slip condition” holds, meaning that the velocity of the gas at a wall is the same as that of the wall (continuum regime); on the other hand, when  $0.001 < Kn < 10$ , the flow analysis must take into account the molecular interactions between the fluid and the wall. In closed channels, this can be done by associating a “slip condition” (meaning that there will be a measurable difference between the fluid velocity at the wall and the wall itself) to the Navier-Stokes equations.

The analysis of the flow resistance through microchannels can be performed using the Darcy Law, which describes the flow of a fluid through a porous medium; it was originally formulated for liquid flows, but it was later extended to gases in the form called compressible Darcy Law, which assumes a continuum regime and the no-slip condition; the equations we discuss in Par. 2.3 are derived from this law. Though, when the size of the channels becomes very small,  $Kn$  grows and can reach a

value beyond 0.001; an extension of the Darcy law was developed by Knudsen considering the slip condition; this is the formulation we use in par. 2.4.

## 2.3. Compressible Darcy law

Assuming one dimensional gas flow, the differential form of Darcy’s Law is given by [2]:

$$N = -\frac{B_v}{\eta} \frac{p}{R^* T} \frac{dp}{dx} \quad (1)$$

If, further, the flow is isothermal and steady, the developments described in [1] can be performed with some adaptations; the main modification lies in the fact that, for the applications described in the present paper, the flow rate of interest is measured/employed downstream, therefore the downstream conditions are of more interest. we will thus write that:

$$pV = p_2 v_2 \quad (2)$$

The (average) velocity downstream of the leak is:

$$v_2 = \frac{Q_V}{A_{ex}} \quad (3)$$

one thus obtains the following equation, which is equivalent to eq. (8) in [1], as reformulated for the aims of the present work:

$$Q_V = \frac{A_{ex} B_v}{2\eta L} \left( \frac{p_1^2 - p_2^2}{p_2} \right) \quad (4)$$

Now, since the flow rate in SCCM is:

$$Q_{SCCM} = Q_V \frac{\rho}{\rho_{ref}}$$

one gets:

$$Q_{SCCM} = \frac{p_2 T_{ref}}{p_{ref} T_2} \frac{A_{ex} B_v}{2\eta L} \left( \frac{p_1^2 - p_2^2}{p_2} \right) = \frac{T_{ref}}{T_2} \frac{A_{ex} B_v}{2\eta L} \left( \frac{p_1^2 - p_2^2}{p_{ref}} \right) \quad (5)$$

It can be seen from this equation that the flow rate in SCCM depends on the difference of the squares of the pressures upstream and downstream of the leak, on the flowing gas through its viscosity, on geometrical parameters ( $A_{ex}$  and  $L$ ) and on the viscous permeability of the leak  $B_v$ ; the last three quantities can be considered as specific properties of the leak and, although they should be nominally the same for all leaks of a same model, they are quite variable due to uncertainties in the fabrication process and very difficult to measure directly to the accuracy required for a precise forecast of the leak properties. On the other hand, these parameters guarantee the stability of the leak response because they are all related to the mechanical structure of the sensing element which, once positioned in the holder, will not undergo variable mechanical stresses. It has to be observed that the permeability might be modified by obstruction of the channels due to dust or other pollutants crossing the device, but this point is outside the scope of the present paper.

Also notice that  $A_{ex}$ ,  $L$  and possibly  $B_v$  might change due to thermal dilatation if the leak is subjected to temperature variation; this effect will of course depend on the material, but it is expected to be repeatable and can therefore be taken in consideration during calibration of the leak.

## 2.4. Knudsen’s expression

As discussed in Par. 2.2, this formulation stems from the expression proposed by Knudsen for predicting gas flows in all regimes, as explained in [2], where it is also shown how, for sufficiently high pressures, Knudsen’s expression can be simplified to the form:

$$N = - \left( \frac{R^2}{8\eta} \frac{p_1 + p_2}{2} + D^k \frac{c_1^k}{c_2^k} \right) \frac{1}{R_g T} \frac{p_2 - p_1}{x_2 - x_1} \quad (6)$$

From this equation and performing developments similar to the ones described in [11], one gets to the equation (18) of [1] which, when expressed as a function of  $Q_V$ , becomes:

$$Q_V = \frac{A_{ex} B_v}{2\eta L} \left( \frac{p_1^2 - p_2^2}{p_2} \right) + 0.89 \frac{d_p^{eff}}{3L} \sqrt{\frac{8R^* T}{\pi M}} \left( \frac{p_2 - p_1}{p_2} \right) \quad (7)$$

And, when expressed as a function of the flow rate in SCCM:

$$Q_{SCCM} = \frac{T_{ref}}{T_2} \frac{A_{ex} B_v}{2\eta L} \left( \frac{p_1^2 - p_2^2}{p_{ref}} \right) + 0.89 \frac{T_{ref}}{T_2} \frac{d_p^{eff}}{3L} \sqrt{\frac{8R^* T_2}{\pi M}} \left( \frac{p_1 - p_2}{p_{ref}} \right) \quad (8)$$

Notice that the first term in eq. (8) is the same as eq. (5), so that its second term can be considered as a correction, which should become vanishing as the slip effects decrease.

Of course, the same considerations described in the last part of par. 2.3 hold here, just by adding  $d_p^{eff}$  to the list of the geometrical parameters.

### 2.5. Determination of the constants

It can be observed that, with the exception of the thermodynamic conditions and the gas properties, both in eq. (5) and in eq. (8) all values are either constants or properties of a given leak (possibly depending on the thermodynamic conditions). It will then be possible to reformulate these equations as follows (where the reference conditions were included in the values  $\alpha'$ ,  $\alpha$  and  $\beta$ ):

$$Q_{SCCM} = \frac{\alpha'}{\eta} \left( \frac{p_1^2 - p_2^2}{T_2} \right) \quad (5b)$$

$$Q_{SCCM} = \left[ \frac{\alpha}{\eta} \left( \frac{p_1^2 - p_2^2}{T_2} \right) + \beta \sqrt{\frac{R^* T_2}{M}} \left( \frac{p_1 - p_2}{T_2} \right) \right] \quad (8b)$$

If the thermodynamic conditions and the flow rate are measured, it will then be possible to determine the values of  $\alpha$  and  $\beta$  for a specific leak.

Specifically, in the case of eq. (8b), it will be possible to write:

$$\frac{Q_{SCCM} T_2}{p_1 - p_2} = \frac{\alpha}{\eta} (p_1 + p_2) + \beta \sqrt{\frac{R^* T_2}{M}} \quad (8c)$$

In order to isolate the value  $\beta$ , we will write:

$$\frac{Q_{SCCM} T_2}{\sqrt{\frac{R^* T_2}{M}} (p_1 - p_2)} = \frac{\alpha}{\eta \sqrt{\frac{R^* T_2}{M}}} (p_1 + p_2) + \beta \quad (8d)$$

For uniformity, we will also reformulate eq. (5b) as follows:

$$\frac{Q_{SCCM} T_2}{\sqrt{\frac{R^* T_2}{M}} (p_1 - p_2)} = \frac{\alpha'}{\eta \sqrt{\frac{R^* T_2}{M}}} (p_1 + p_2) \quad (8c)$$

The use of eqs. (5c) and (8d) in calibration and application of the leaks will be discussed in the following paragraphs. Notice that similar expressions can easily be obtained also for the volumetric flow rate  $Q_V$ , but in this paper we chose to work with the standardized flow rate  $Q_{SCCM}$  due to its wide use in practical applications.

## 3. Experimental setup

### 3.1. Dataset

Test were performed using four ATEQ flow leaks (type A, type 5, type D and type E), which were mounted in series upstream of the reference test rig. The upstream pressure was regulated by a Druck PACE 5000 pressure regulator, which allows to obtain relative pressures up to 7 bar

with a stability of approximately 10 Pa; the downstream pressure was set at the ambient pressure (see par. 3.2).

Fig. 1 displays a picture of the experimental setup that was used; the different components of the experiment, described in the following, are indicated by letters in the figure.

For more clarity, the system is described in the architectural scheme reported in Fig. 2.

Leaks were tested at various nominal differential pressures as reported in Table 1.: all measurements were performed considering a reference temperature of 20 °C (293.15 K) and a reference pressure of 101325 Pa (1 atm) for the definition of the standard flow rate.

As can be seen, a few cases had to be excluded from the analysis; this was done because in those cases the measurements were not considered reliable due to excessive pressure drops between the pressure port and the leak, or insufficient pressure stability; we are currently preparing an improved setup which was designed to overcome such limits.

### 3.2. Reference measurement

The flow rate from the leaks was measured using INRIM high accuracy piston prover MICROGas, fully described in previous works [3,4]. The rig is a piston of the plunger type, whose movement is controlled by a feedback system programmed to keep the internal pressure of the piston to a predetermined level; in the present work, this pressure level was set at ambient pressure. The test rig measurement capability ranges between 0.1 and 1200 SCCM, with an uncertainty of 0.05%.

The piston is in a laboratory whose temperature is controlled to within 0.1 K, while the temperature inside the piston is kept constant to within 0.02 K; both temperatures were set to 20 °C nominal for the experiments described in the present paper.

Calibration measurements were performed by measuring the flow rate provided by the leak under test at the various pressures, and repeating every measurement three times.

Such data were elaborated according to the analysis presented in Par. 2, developing both the baseline Darcy law and the more complex Knudsen-modified Darcy law; the outcomes of the two equations could be compared based on the calibration results (see par. 4).

### 3.3. Thermodynamic data

Pressures and temperatures were measured using the instruments (Barometer RUSKA type 6200, thermometer Corradi RP7000) associated to the MICROGas test rig; both instruments are traceable to the respective National Standards, and the uncertainty associated to their

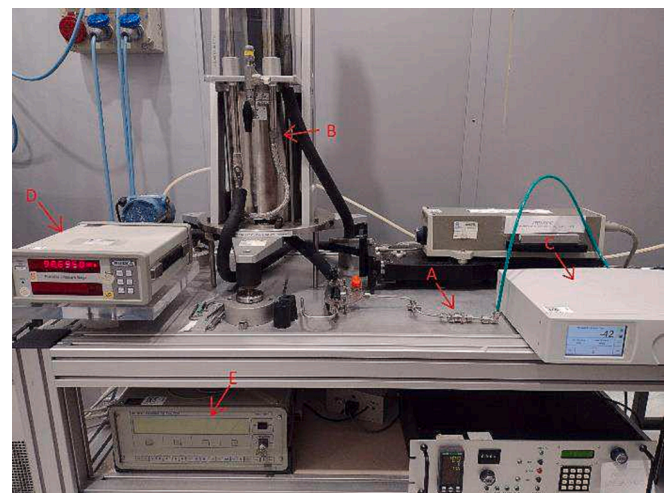
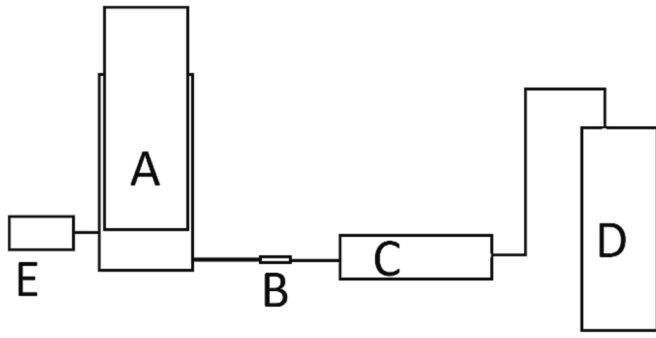


Fig. 1. Experimental setup. A: Flow leak; B: reference piston prover; C: pressure regulator; D: Barometer; E: Thermometer.



**Fig. 2.** Architecture of the system. A: Reference flow measurement (piston prover); B: leak; C: Pressure regulator and upstream pressure measurement; D: Gas Source (bottle); E: Barometer measuring the pressure in the piston (downstream pressure, see 3.3).

**Table 1**

Test pressures.

Test #	Nominal differential pressure (mbar)	Leak tested			
		A	S	D	E
1	100	NO	X	X	X
2	300	X	X	X	X
3	500	X	X	X	X
4	850	X	X	X	X
5	1000	X	X	X	X
6	2000	X	X	X	NO

measurements is of 4 Pa and 0.01 K respectively.

The sensor (PT100 probe) connected to the thermometer is placed inside the piston prover (A in Fig. 2); due to the stabilized ambient temperature, it is assumed that the temperature inside the piston is the same as the temperature at the leak exit. Also, due to the very low flow rates employed, pressure losses in the tubing are negligible, thus the pressure at the leak exit can be assumed to be equal to the pressure inside the piston.

The viscosity, which is required within the computations, was computed by applying Sutherland's law to the temperature measured downstream of the leak.

#### 4. Calibration results

Based on Eqs. (5c) and (8d), data collected during calibrations were plotted on Cartesian graphs using the following variables:

$$X = \frac{(p_1 + p_2)}{\eta \sqrt{\frac{R^* T_2}{M}}}; Y = \frac{Q_{SCM} T_2}{\sqrt{\frac{R^* T_2}{M}} (p_1 - p_2)} \quad (9)$$

Results thus obtained are presented in Figs. 3a-3d.

##### 4.1. Elaboration according to eq. (8d)

As can be observed in Fig. 3(a) to 3(d), data are aligned along straight lines. This is in accordance with the theoretical predictions of Eq. (8d), which has the general form  $Y = \alpha X + \beta$ . It is therefore possible to determine the values of  $\alpha$  and  $\beta$  through a simple linear regression analysis on the data.

The calibration process is described graphically in the block diagram reported in Fig. 4.

The resulting parameters for the four leaks under test are reported in Table 2:

It can be observed that the values of  $\alpha$  and  $\beta$  display a growing behaviour as the leak nominal flow rate increases, which is coherent with the expected result. Indeed, considering two leaks with different permeability, for a given pressure difference it is expected that the flow

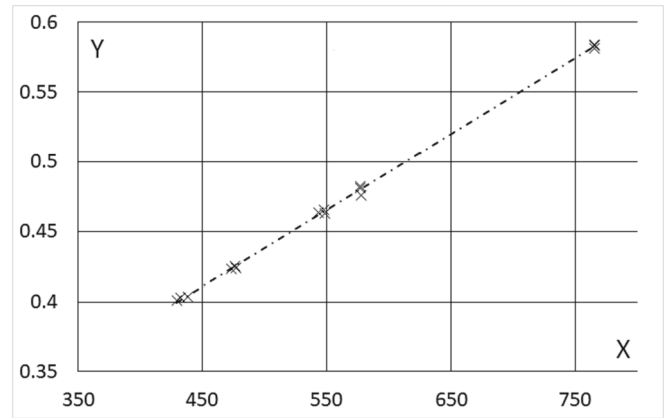


**Fig. 3a.** Calibration of Leak A.

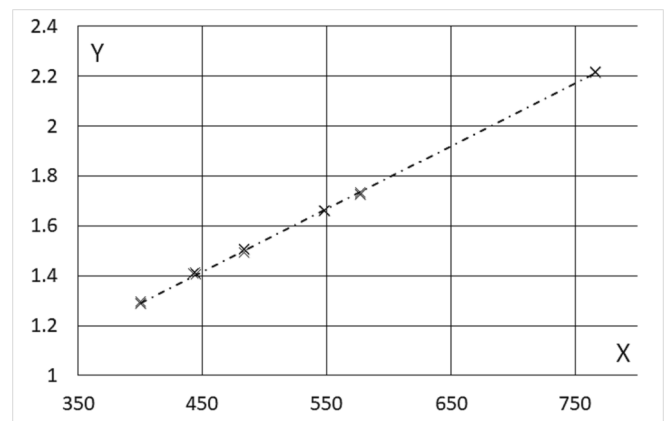


**Fig. 3b.** Calibration of Leak 5.

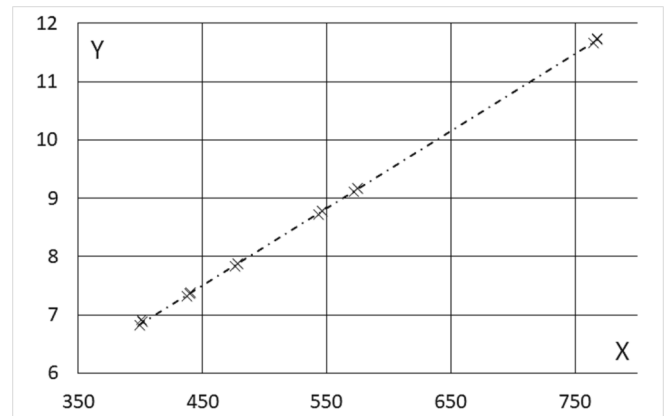


**Fig. 3c.** Calibration of Leak D.

rate will be higher and grows more quickly with pressure. Also notice that the relative importance of the constant term reduces as the nominal flow rate of the leak increases; this fact will be analysed in more detail in 4.2.

##### 4.2. Elaboration according to eq. (5c)

When data are analysed according to Eq. (5c), it must be observed that this equation assumes a direct proportionality between the values of  $X$  and  $Y$ ; this means that every calibration point must be analysed

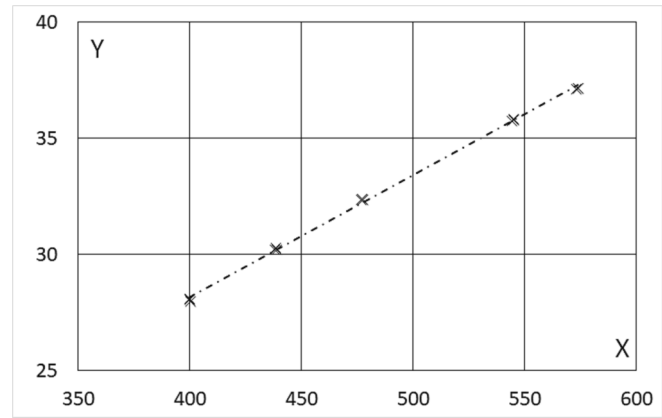


Fig. 3d. Calibration of Leak E.

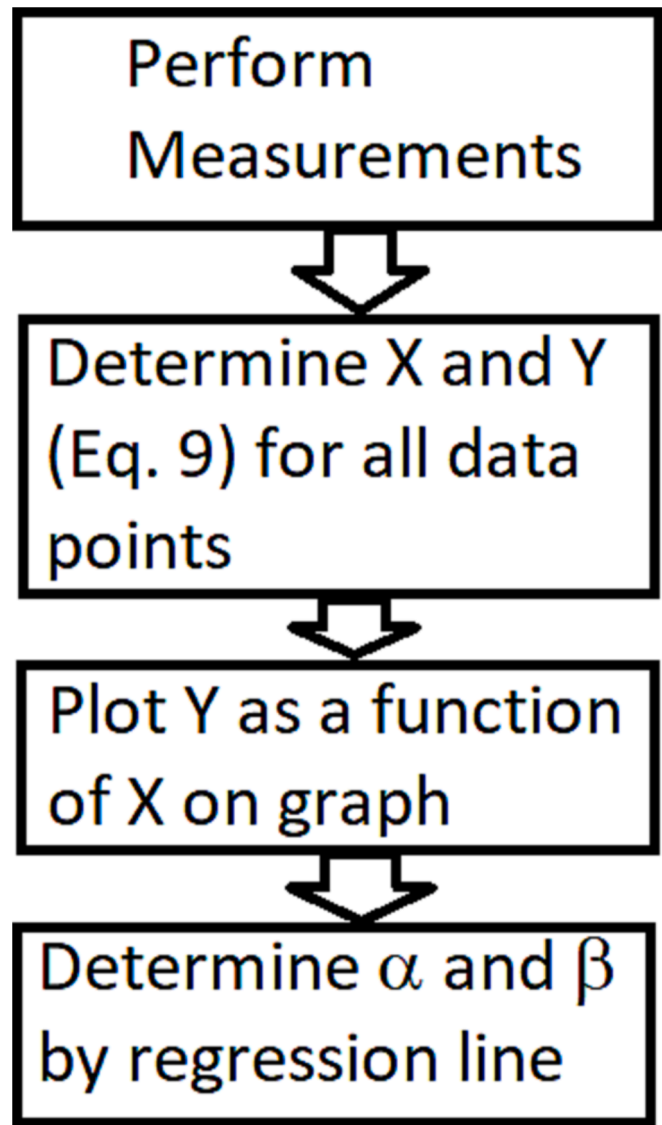


Fig. 4. Block diagram of the calibration process.

separately in this case, to determine the ratio  $\alpha' = Y/X$ . We will then plot graphs of the value of  $\alpha'$  as a function of  $X$  (Figs. 5a-5d), from which it will be possible to deduce the evolution of the proportionality ratio as a function of the pressure level. Physically, the result that the value of  $\alpha'$  is

Table 2  
Regression equations for the four leaks.

Leak	Equation
A	$Y = 0.0005446X + 0.1657507$
5	$Y = 0.002513X + 0.286205$
D	$Y = 0.013234X + 1.555687$
E	$Y = 0.052447X + 7.186322$

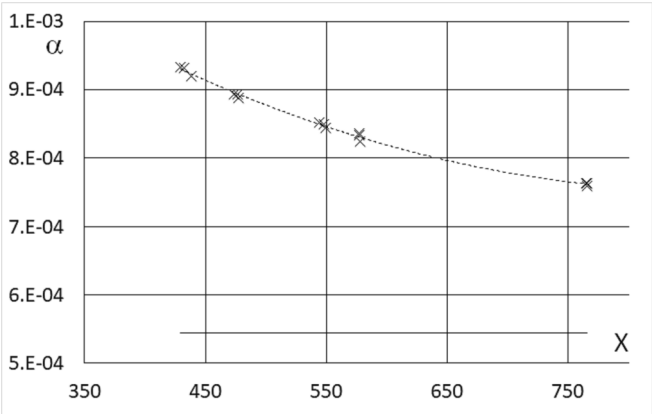


Fig. 5a. Comparison of Eq. (5) to Eq. (8), Leak A.

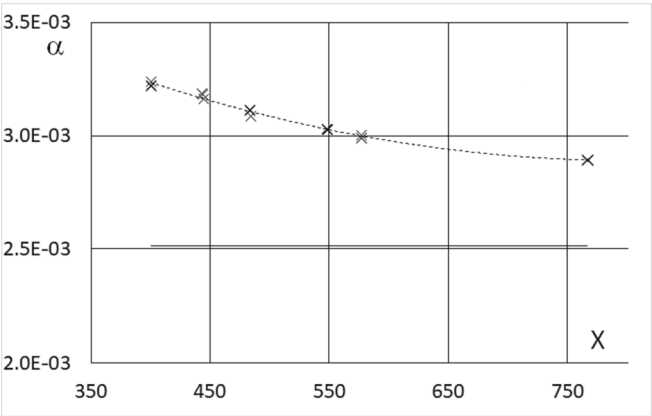


Fig. 5b. Comparison of Eq. (5) to Eq. (8), Leak 5.

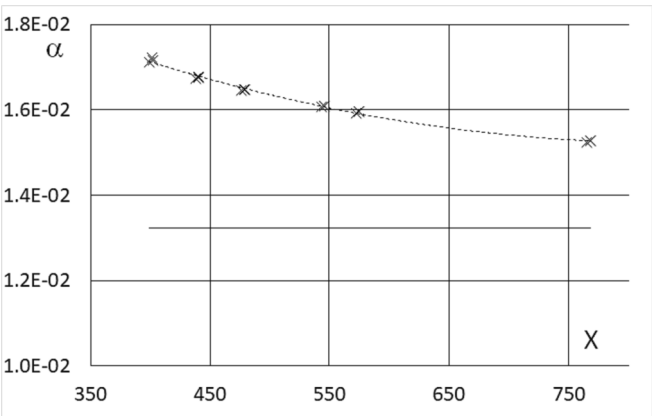


Fig. 5c. Comparison of Eq. (5) to Eq. (8), Leak D.



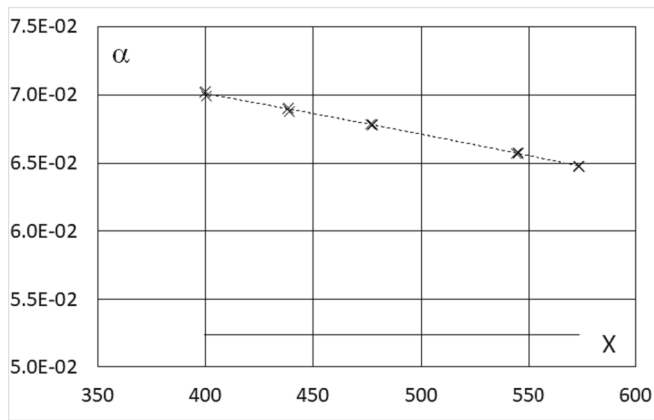


Fig. 5d. Comparison of Eq. (5) to Eq. (8), Leak E.

not constant expresses the fact that the simple compressible Darcy law is not exactly valid, i.e. that in the range analysed here the leaks employed undergo the effect of the slip condition described in 2.3.

Figs. 5a-5d also include an horizontal line, which represents the value of  $\alpha$  obtained in par. 4.1, and is of course constant with the pressure.

It can be observed that, in all cases, the behaviour of  $\alpha'$  tends to the value of  $\alpha$  following a clear and repeatable trend, which can therefore be interpolated through regression analysis. This implies that it is also possible to apply Eq. (5) for the determination of the flow rate, with a method similar to what will be shown in Par. 4.3, by computing  $\alpha'$  from the relevant interpolation equation. We do not feel, though, that this approach should be recommended, because the small reduction in complexity for the elaboration in the results would be more than offset by the requirement of more calibration datapoints, necessary for a correct determination of the functions in Fig. 5, and the further complexity in the determination of the interpolation equation.

It is also possible to notice that the relative differences between  $\alpha'$  and  $\alpha$  tend to diminish as the nominal flow of the leak increases; this fact is coherent with the observation that the leaks with lower flows imply smaller passages for the gas and therefore an increase of the molecular effects. On the same line of thought, the reduction in importance of the constant term  $\beta$  described in 4.1 indicates a reduced importance of the molecular effects as the nominal flow rate increases.

#### 4.3. Application in use

In order to check the validity of the calibration of the leaks, we performed a few tests of application; specifically, we applied various differential pressures (different from the calibration pressures, but within the interpolation range) to leak D, in slightly different ambient conditions than the ones encountered in calibration.

Since the relevant conditions (pressures, temperatures) were also measured, it was possible to determine the value of  $X$  and, by applying the equation for leak D reported in Table 2, to compute the value of  $Y$ ; inverting then the definition of  $Y$ , it was possible to compute the flow rate in SCCM, as described in the block diagram reported in Fig. 6.

For testing purposes, the reference flow rate was also measured as described in par. 3, so that it was possible to compare the flow rate obtained from Eq. (8d) to the reference one; it was therefore possible to compare these flows. Results of such tests are reported in Table 3.

It can be observed that, in all cases, the difference is very small, thus confirming that the proposed rescaling of the quantities of interest allows to obtain an excellent accuracy in the computation of the flow delivered by the leak.

In particular, in all but one case the relative difference between the measured and computed flow is within the uncertainty of the reference test rig, thus indicating that the two results are fully consistent. The first

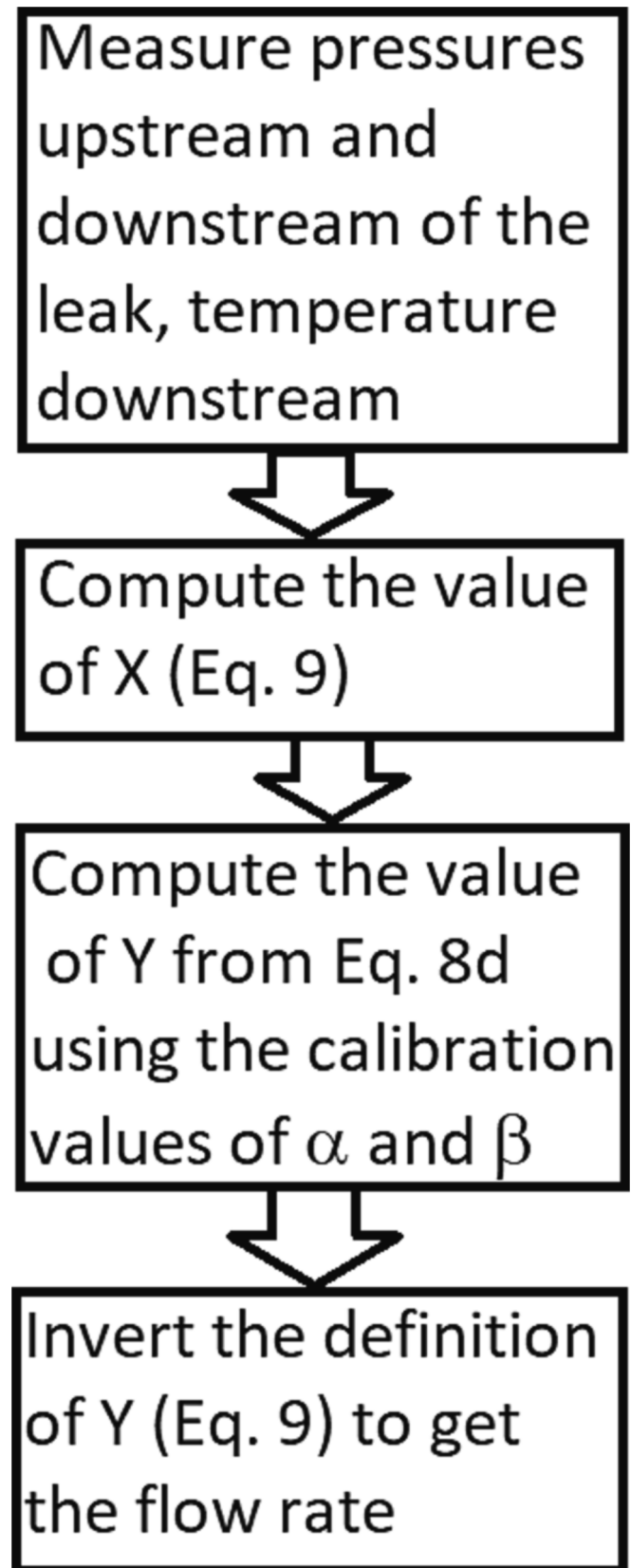


Fig. 6. Block diagram of in-use application of Eq. (8d).

**Table 3**  
in-use tests, leak D.

Nominal differential pressure (mbar)	Measured flow (SCCM)	Computed Flow (SCCM)	Difference, %
200	1.429	1.427	0.17
400	3.066	3.065	0.05
900	8.033	8.029	0.05
1500	15.663	15.657	0.04

case, on the other hand, refers to a very small pressure difference, which as stated earlier is considered as less reliable with the present experimental setup due to not fully satisfactory stability of the pressure difference.

## 5. Conclusions and future work

An improved way of rescaling the flow delivered by a flow leak was proposed; it was shown that the proposed model allows to obtain excellent calibration curves, which in turn lead to a very good accuracy in the computation of the delivered flow for applications.

The main advantage of the proposed model is its insensitivity to ambient pressure conditions, which with the previous approach could cause deviations in the computation of the flow delivered by the leak depending on pressure variations.

The model also takes into account the effects of temperature, by considering the value  $T_2$  (temperature downstream of the leak) in Eq. (8d) and (5c); though, it may be difficult to measure this value in practical application; in our experimental setup, we assumed that this temperature is the same as the one of the gas collected in the reference test rig; indeed, this assumption is quite strong and can be considered valid only in laboratory applications at low flow rates, where the ambient is at a constant temperature and the friction heating of the leak is negligible; a possible solution, which we intend to investigate, is to measure directly the temperature of the leak. Of course, this still implies to assume isothermality of the leak, but this assumption is much weaker considering the thermal conductivity of the metal used for the construction of the leaks.

Additionally, our model takes into account the effect of the working

gas through its molar mass and viscosity (Eq. (8d) and (5c)), so calibration of a leak with one gas should be valid for any working gas provided these values are known.

The analysis discussed in the present paper will be used in the design of a transfer standard (TS) for flow comparisons, which we expect will provide very good stability properties due to the discussed insensitivity to the ambient pressure.

## CRedit authorship contribution statement

**Pier Giorgio Spazzini:** Conceptualization, Formal analysis, Software, Supervision, Writing – original draft, Writing – review & editing. **Gaetano La Piana:** Methodology, Investigation. **Aline Piccato:** Conceptualization, Formal analysis. **Vittorio Delnegro:** Formal analysis, Software, Investigation, Data curation. **Massimo Viola:** Formal analysis, Software, Investigation, Data curation.

## Declaration of Competing Interest

The authors declare that they have no known competing financial interests or personal relationships that could have appeared to influence the work reported in this paper.

## Data availability

Data will be made available on request.

## References

- [1] N.B. Carrigy, L.M. Pant, S. Mitra, M. Secanell, Knudsen diffusivity and permeability of PEMFC microporous coated gas diffusion layers for different polytetrafluoroethylene loadings, *J. Electrochem. Soc.* 160 (2013) F81–F89.
- [2] R.E. Cunningham, R.J.J. Williams, *Diffusion in gases and porous media*, Plenum Press, New York, 1980.
- [3] G. Cignolo, F. Alasia, A. Capelli, R. Gorla, G. La Piana: “A Primary Standard Piston Prover for Measurement of Very Small Gas Flows”, *Proceedings of the 5<sup>th</sup> ISFFM*, Arlington, Va. (USA), p. 10, 2002.
- [4] P. G. Spazzini, A. Piccato, P. Pedone: “Reduction of a Gas Prover Uncertainty”, *Proceedings of the 10<sup>th</sup> ISFFM*, Querétaro. (Mexico), 2018.
- [5] G.A. Bird, *Molecular gas dynamics and the direct simulation of gas flows*, Clarendon Press, Oxford, 1994.